ACS Sustainable Chemistry & Engineering

pubs.acs.org/journal/ascecg

Research Article

Combining Associative and Dissociative Dynamic Linkages in Covalent Adaptable Networks from Biobased 2,5-Furandicarboxaldehyde

Matteo Andrea Lucherelli, Antoine Duval,* and Luc Averous*

Cite This: *ACS Sustainable Chem. Eng.* 2023, 11, 2334−2344

Read Online

ACCESS | Metrics & More | Article Recommendations | Supporting Information

ABSTRACT: Covalent adaptable networks (CAN) emerged as a recent class of polymers that combine the most interesting advantages of thermosets and thermoplastics. In this frame, combining different dynamic linkages within the polymer network could be an interesting approach to finely tune the material properties and determine the extent of their behaviors. Here, we report the synthesis of novel dually crosslinked CAN in which dynamic associative imine linkages and dissociative Diels−Alder adducts were both obtained by exploiting the chemistry of a single biobased building block, 2,5-furandicarboxaldehyde (FDC). Thanks to the favorable chemical environment of the furan ring in a linear polyimine based on FDC, very fast coupling with maleimides in Diels−Alder reactions was reported, leading to the formation of polymer networks in remarkably short times. The obtained sustainable polymer systems were shown to have a behavior in-between those of vitrimers and dissociative CANs, with tunable mechanical behavior and excellent reprocessability.

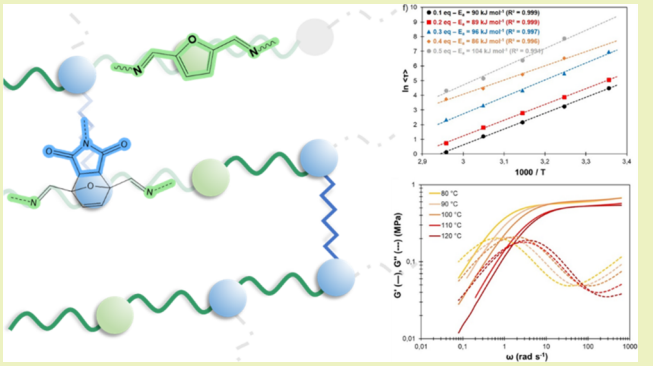

KEYWORDS: *covalent adaptable networks, vitrimer, imine, Diels−Alder, 2,5-furandicarboxaldehyde, 2,5-diformylfuran*

INTRODUCTION

Polymer materials are commonly classified into two main categories: thermoplastics and thermosets. Thermosets present excellent mechanical properties and stability compared to thermoplastics, but unlike the latter, thermosets cannot melt upon heating, which prevents them from being easily reshaped and recycled. Covalent adaptable networks (CANs) emerged in the past 20 years as a new class of polymer materials, which are able to bridge the gap between thermosets and thermoplastics by combining the advantages of both worlds.[1−4] CANs contain dynamic covalent bonds in their structures, permitting a rearrangement of the network under external stimuli, such as temperature or light radiation.

CANs are separated into two different categories, depending on the mechanism of bond exchange.[5] In dissociative CANs, bonds are first broken before being reformed in another position. The network thus passes by a state with reduced connectivity or can even be completely depolymerized. Associative CANs, also known as vitrimers, rely on the opposite of bond exchange with maintained connectivity.[6] The network crosslink density remains constant throughout the bond exchange process, retaining its structural integrity. First examples of vitrimers were based on transesterification exchange reactions,[7−9] but since then several different dynamic covalent associative bonds have been introduced.[10,11] However, the frontier between associative and dissociative mechanisms is sometimes difficult to draw.[12,13]

CANs have received considerable attention in the past few years for their peculiar properties, such as stimuli−responsiveness and self-healing, allowing for promising applications, for use in tunable devices, soft robots, or car industry, among others.[14−16] In addition, the reversibility of the covalent network allows to reprocess or recycle thermoset-like architectures, potentially increasing their sustainability and reducing end-of-life plastic waste.[17,18] In the frame of circular bioeconomy, the combination of circularity with the development of biobased polymers should help to reduce the environmental impact of polymer materials.[19] Important properties of CANs, such as their reprocessability, depend on the kinetic of the exchange reaction and its temperature dependence. The use of external catalysts has been the first option to control vitrimers properties,[9,20] followed by several other emergingstrategies,

Received: October 5, 2022
Revised: January 10, 2023
Published: February 2, 2023

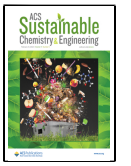

https://doi.org/10.1021/acssuschemeng.2c05956
ACS Sustainable Chem. Eng. 2023, 11, 2334−2344

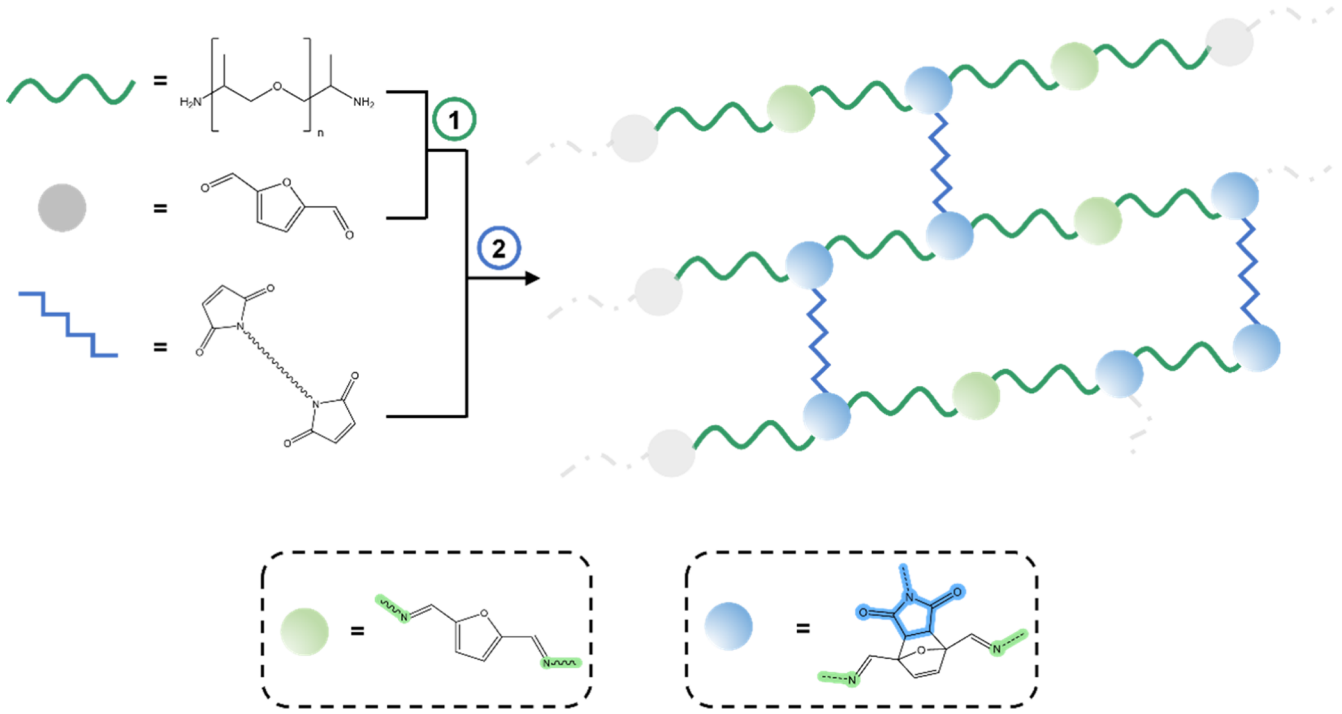

Figure 1. Simplified representation of dual networks synthesis. Spheres represent FDC included in the network, with different colors depending on whether FDC participates in linear PI only (green) or in PI with DA crosslinks (blue).

such as internal catalysis, neighboring group participation,[21] or more generally the precise control of the network architecture.[22]

To further tune the materials' properties and achieve more sophisticated properties, CANs combining two types of exchange mechanisms have also been recently designed.[23] They are often referred to as dual dynamic networks (DDNs).[24] Examples of DDNs combining disulfide bonds with imines,[25,26] hydroxyurethanes,[27] esters,[28,29] or acylhydrazones[30] dynamic linkages have for instance been reported. Boronic esters and boroxines are other kinds of dynamic bonds that have often been used in CANs synthesis.[31−33] They have been employed in the synthesis of DDNs in combination with imines,[34−36] oximes,[37] or acylhydrazones[38] dynamic linkages. Reversible Diels−Alder (DA) reactions are among the most frequently employed dynamic covalent chemistries in polymer science, typically relying on the coupling (DA) and decoupling (retro-DA) of furans with maleimides.[39] DA adducts represent the most evident example of dissociative dynamic linkages, since they are dissociated by retro-DA reaction above 100−120 °C and are (re)-associated usually around 60−80 °C. They have seldom been used in combination with associative dynamic linkages, such as imines[40] or acylhydrazones,[41] to produce DDNs combining both associative and dissociative exchanges.

Recently, our team focused on a promising biobased building block, 2,5-furandicarboxaldehyde (FDC), for the synthesis of biobased polyimine (PI) vitrimers.[42,43] One of FDC precursors, FDCA (2,5-furan dicarboxylic acid), was selected among the 12 top value-added chemicals from biomass by the American Department of Energy (DoE) in 2004.[44] It can be produced by controlled oxidation of 5-(hydroxymethyl)furfural (HMF), using green processes.[45−51] HMF is considered one of the most promising biobased molecules for green chemical approach to polymer synthesis.[52−54]

In this work, we further exploited the peculiar structure of FDC to introduce two kinds of dynamic linkages into CANs (Figure 1). Imine linkages have been obtained by condensation of the aldehyde groups of FDC with the amine end-groups of an oligo-etheramine, as reported before.[42,43] DA crosslinks have been achieved by the reaction of the furan ring with bismaleimides. The chemistry has been assessed by model compound study with NMR and Fourier transformed infrared (FTIR) spectroscopies. The obtained DDN combining associative (imine) and dissociative (DA) exchanges have then been characterized by different complementary approaches including thermal analyses [TGA, differential scanning calorimetry (DSC)], dynamic mechanical analysis (DMA), rheological analyses (stress relaxation and frequency sweeps), and uniaxial tensile tests. Finally, their reprocessability has also been assessed.

EXPERIMENTAL PART

Materials. HMF was purchased from Fluorochem and used as received without further purification. FDC was synthesized from HMF, as previously reported.[55] More information and characterization data are available in the Supporting Information. Oligo-ether-amine (Jeffamine D400, $M_n \approx 430$ g mol^{-1}) was obtained from Huntsman. It is an oligomer composed of about six repeating units of propylene oxide with primary amine groups as chain ends. 4,4′-methylenebis(*N*-phenylmaleimide) (BM) was purchased from Alfa Aesar (Ward Hill, Massachusetts, United States), *N*-methylmaleimide from Acros (Fukuoka, Japan), and NaBr, $MgSO_4$, and butylamine from Sigma-Aldrich.

Synthesis of Linear PI. FDC and oligo-ether-amine were dissolved in THF in equal molar amount, and the mixture was stirred overnight at room temperature. The color of the solution turned from light yellow to dark brown during reaction time. The solvent was then evaporated in a rotary evaporator to give a brown viscous oil, which was further dried in a vacuum oven at 40 °C for 16 h.

Gelation Tests. PI (200 mg, 1 equiv, 0.36 mmol of furane) and BM (58 mg, 0.16 mmol, 0.45 equiv of maleimide moiety) were dissolved in DMSO (1.4 mL) in a glass vial. The mixture was stirred at 80 °C, and the vial was turned upside down at regular intervals to detect the formation of a solid gel.

https://doi.org/10.1021/acssuschemeng.2c05956
ACS Sustainable Chem. Eng. 2023, 11, 2334−2344

Scheme 1. Synthesis of Linear PI

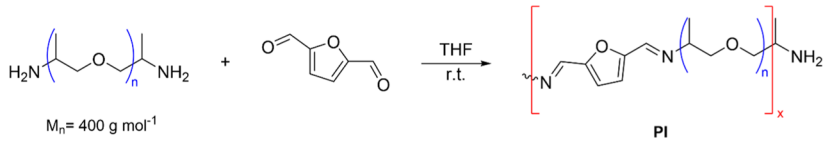

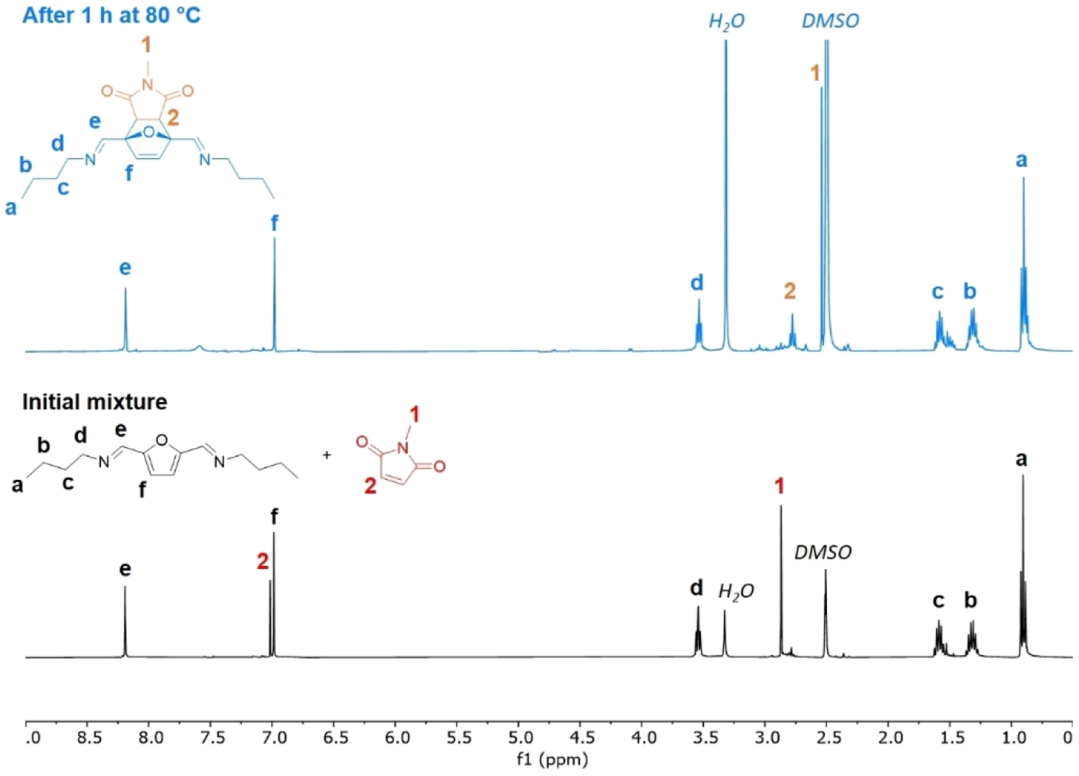

Figure 2. ^{1}H NMR spectra (400 MHz, DMSO-d_6) of the mixture of model compound **1** and *N*-methylmaleimide, immediately after mixing and after 1 h at 80 °C.

General Synthesis of Cross-Linked Polymer Networks (PI-BM-*X*). PI was dissolved in THF, and BM was added to the solution. The mixture was stirred at room temperature for 5 h and then poured in a PTFE mold. The solvent was left to evaporate under a fume hood at room temperature, followed by vacuum drying at 60 °C for 15 h. The material was finally cured in a hot press at 80 °C for 40 min, resulting in a dark brown elastic solid.

Materials Characterizations. FTIR spectra were collected on a Thermo Scientific Nicolet iS10 spectrometer with a diamond ATR probe at room temperature. A total of 32 scans were accumulated at a resolution of 4 cm^{-1}.

NMR spectra were recorded on a Bruker 400 MHz spectrometer at 25 °C. The samples were dissolved in $CDCl_3$, and 16 scans were collected.

Thermogravimetric analyses (TGA) were performed under nitrogen flow (flow rate 25 mL min^{-1}) using a Q5000 IR apparatus from TA instruments. Samples (1−3 mg) were heated from 40 to 700 °C at a heating rate of 10 °C min^{-1}. The temperature at which 95% of the initial weight remains is reported as $T_{95\%}$.

DSC was conducted under nitrogen flow (flow rate 50 mL min^{-1}) using a Discovery DSC 25 apparatus from TA instruments. The sample was first cooled down to −70 °C and then heated up to 200 °C at a heating rate of 10 °C min^{-1}. Then, it was cooled down to −70 °C at a cooling rate of 10 °C min^{-1} and a second heating run was performed under similar conditions. The glass transition temperature (T_g) was measured at slope change from the first heating run.

Rheological tests were performed on a Discovery HR-3 apparatus form TA instruments. The experiments were performed in parallel plate geometry using 25 mm sample disks. For stress relaxation experiments, a normal force of 1 N in compression mode and a strain of 2% were applied to the material. The relaxation modulus $G(t)$ was followed over time at a constant temperature. The series of stress relaxation experiments was performed successively on the same sample. Relaxation modulus was normalized to the value at 1 s (G_{1s}), and data were fitted with a stretched exponential decay.

DMA was carried out in torsion mode on a Discovery HR-3 apparatus from TA instruments using rectangular samples (about 16 mm × 5 mm × 1 mm). Measurements were taken from −60 to 110 °C with a heating rate of 2 °C min^{-1}. The axial force was constantly adjusted to 1 ± 0.5 N. The applied strain was 0.05% at an oscillating frequency of 1 Hz. Storage and loss modulus, G' and G'', were collected as a function of temperature. The relaxation temperature T_α was taken at the maximum of tan $\delta = G''/G'$.

Uniaxial tensile tests were also performed on a Discovery HR-3 apparatus form TA instruments. The dumbbell-shaped samples had an effective length of 14 mm, a width of 4.5 mm, and a thickness of about 1 mm. The tensile measurements were performed at room temperature, using a preload of 0.05 N and pulling speed of 50 μm s^{-1} until sample failure. Reported values (elongation at break, tensile strength, and Young's modulus) are averages of at least four experiments with their corresponding standard deviations. The plotted tensile curves were selected to be representative of the average values.

Reprocessability was performed by cutting the samples into small pieces (<2 mm), which were placed into the dumbbell-shaped mold used for tensile test and pressed at 80 °C for 40 min. Uniaxial tensile tests were used to follow the evolutions of the material properties before and after each reprocessing cycle.

https://doi.org/10.1021/acssuschemeng.2c05956
ACS Sustainable Chem. Eng. 2023, 11, 2334−2344

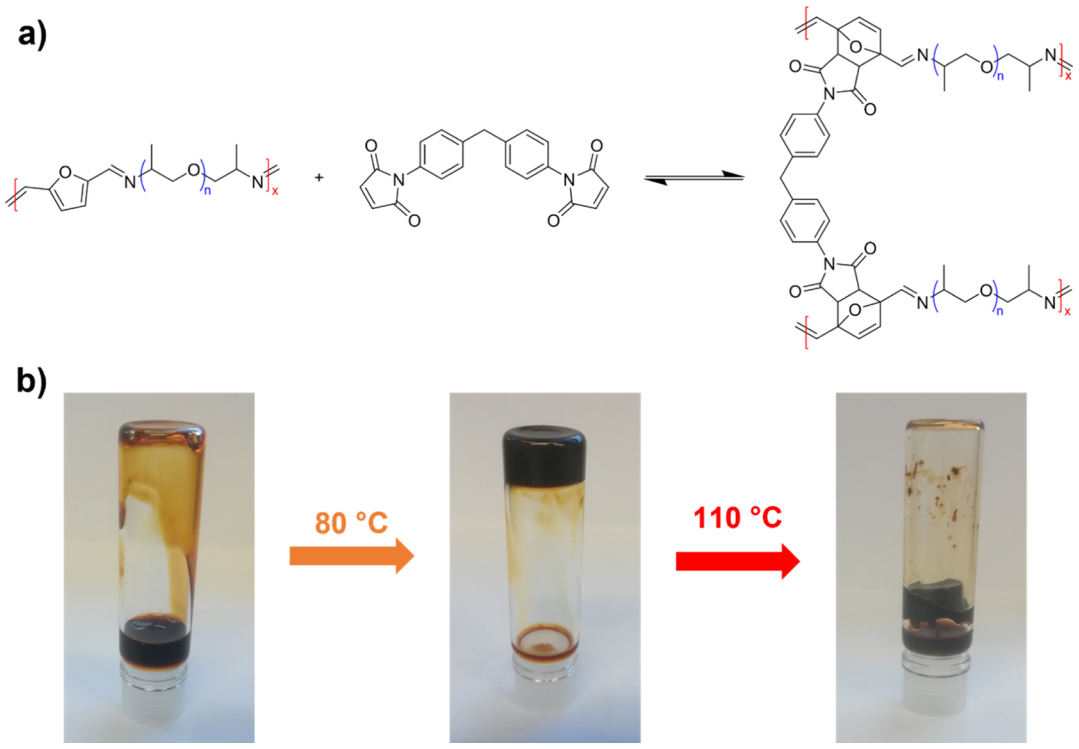

Figure 3. Scheme and picture of gelation tests: (a) scheme of the chemical reaction between PI and BM to form crosslinked polymer networks; (b) photos of first solution in DMSO, gel formation at 80 °C, and partial disruption of the gel at 110 °C.

RESULTS AND DISCUSSION

Synthesis of Dually Crosslinked CANs with Imine and DA Dynamic Bonds. A linear PI was first synthesized by polycondensation between a oligo-ether-amine and the biobased building block FDC (Scheme 1). It has already been employed for the synthesis of PI vitrimers with various polyamines.[42,43] The reaction was performed at room temperature by simply stirring the two reagents in THF in a stoichiometric ratio between amine and aldehyde groups, followed by solvent evaporation. The polymerization was assessed by ^{1}H NMR (Supporting Information, Figure S4), which shows the disappearance of the aldehyde peak at 9.6 ppm and the appearance of a peak at 8.1 ppm corresponding to the imine linkage. FTIR confirms the formation of the imine linkage, with the appearance of a characteristic band at 1636 cm^{-1} related to C═N stretching (Figure S5). ^{13}C NMR further confirms the expected structure of PI (Supporting Information, Figures S6).

The obtained PI present furan groups surrounded by two imine linkages (Scheme 1). To determine whether these structures are suitable for DA reactions with maleimides, a model compound study was first performed. Model compound **1** obtained by the condensation of FDC with 1-pentyl amine (Figure 2, Scheme S2 and Figure S2. See Supporting Information for the synthesis), which mimics the PI structure, was reacted with *N*-methylmaleimide in DMSO-d_6, and the reaction was followed by ^{1}H NMR (Figure 2). After only 1 h stirring at 80 °C, ^{1}H NMR showed the complete disappearance of the maleimide peak at 7.00 ppm (labeled as **2** in Figure 2), and the shift of the peak related to the methyl group of maleimide (labeled as **1** in Figure 2) from 2.86 to 2.53 ppm, as reported by Froidevaux et al.,[56] confirming the occurrence of the reaction.

The reaction between PI and *N*-methylmaleimide showed the same trend, with the disappearance of the maleimide peak at 7 ppm (Supporting Information, model compound **3**, Figure S3). Then, the reaction with BM quickly led to the formation of a gel, in only 2 h at 80 °C (Figure 3b). This reaction time is very short compared to most reported systems, for which up to 24 h were necessary to obtain gels.[57,58] DA reactions, especially furan-maleimide coupling, are commonly used to produce CANs because of their suitable green chemical approach to polymer synthesis.[39,59,60] Furan-based DA reactions are normal-electron-demand reactions, involving electron-rich dienes and electron-deficient dienophiles.[61] Maleimides are among the most reactive dienophiles because of their bisactivation by C═O groups and their cyclic structure, making them widely used in combination with furans. The influence of the substituents on the furan ring on the reactivity in DA reactions has been investigated by several authors for the synthesis of small molecules,[61] as summarized by Khan et al., using density functional theory simulations.[62] In this system, the high reactivity can be explained by the presence of two electron-donating imine groups surrounding the furan rings.

The retro-DA reaction was shown after heating at 110 °C for 12 h. However, the gel was only partially disrupted in these conditions, as shown in Figure 3b. Indeed, the retro-DA of endo adducts is known to occur at higher temperature,[56] as later confirmed by DSC (Figure 5), which can explain that the retro reaction is incomplete here. However, increasing the temperature did not help to further disrupt the gel, probably because maleimide homopolymerization can happen as side reaction, leading to the formation of permanent crosslinks.[63]

Finally, crosslinked networks were produced by reaction between PI and BM as dienophile for DA reaction (Figure 1). Five materials were produced by varying the amount of BM from 0.1 to 0.5 M equiv (labeled as PI-BM-*X*, where *X* is the molar amount of BM).

FTIR was conducted on the obtained materials and compared to neat BM (Figure 4). The peak at 1700 cm^{-1}, corresponding to C═O of maleimide present a redshift to 1716 cm^{-1}, imputable

https://doi.org/10.1021/acssuschemeng.2c05956
ACS Sustainable Chem. Eng. 2023, 11, 2334−2344

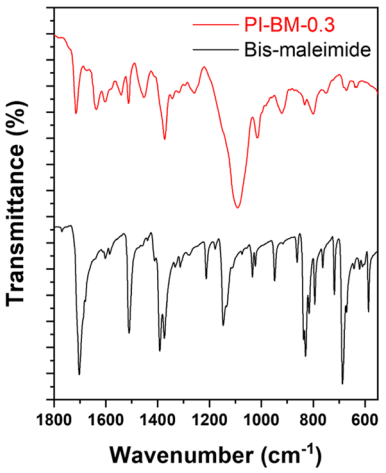

Figure 4. FT-IR spectra comparison of PI-BM-0.3 and BM.

to maleimide structure modification. Moreover, peaks at 826 and 686 cm^{-1} corresponding to maleimide C=C bending disappeared, confirming the formation of the DA adducts.[57]

Thermal and Physical Properties of the Dually Crosslinked CANs. The thermal stability of the networks was studied by TGA (curves are available in the Supporting Information, Figure S7). All materials showed good thermal stability, with a $T_{95\%}$ above 220 °C (Table 1). Increasing the amount of BM

Table 1. Thermal Properties of the Dually Crosslinked Networks

	TGA			DSC	DMA
Material	$T_{95\%}$ (°C)	T_d (°C)	m_{res} (%)	T_g (°C)	T_α (°C)
PI-BM-0.1	220	373	21.5	−22	−16
PI-BM-0.2	229	383	22.2	−19	−9
PI-BM-0.3	235	389	23.9	−18	−6
PI-BM-0.4	243	387	25.2	−19	4
PI-BM-0.5	244	388	26.9	−19	9

leads to an increase in the $T_{95\%}$ as well as in the residual mass at 700 °C (Figure S8) because of an increased aromatic content. All the materials show a main degradation peak around 370−390 °C (Figure S7), which is related to the degradation of the oligo-ether-amine constituting the linear PI.

Considering the TGA results, the materials were then analyzed by DSC between −80 and 200 °C. The DSC traces of PI-BM-0.3 are shown on Figure 5. The traces for the other materials are given in Supporting Information (Figure S9). All the networks showed similar thermal behaviors, with a T_g around −20 °C, which appears to be independent on the level of crosslinking with BM (Table 1). The fact that it does not vary with the introduction of BM can be the sign of a phase separation in the materials, where the T_g at low temperature would be related to only one particular phase. This kind of behavior is commonly observed in, for example, thermoplastic polyurethanes, in which soft segments that are separated from the hard segments present a T_g at low temperature.[64] In the developed systems, phase separation could potentially occur between "soft segments" constituted by the long oligo-ether backbone and "hard segments" constituted by the aromatic furan and/or the rigid DA adducts formed with BM. Further analyses would, however, be needed to confirm this hypothesis.

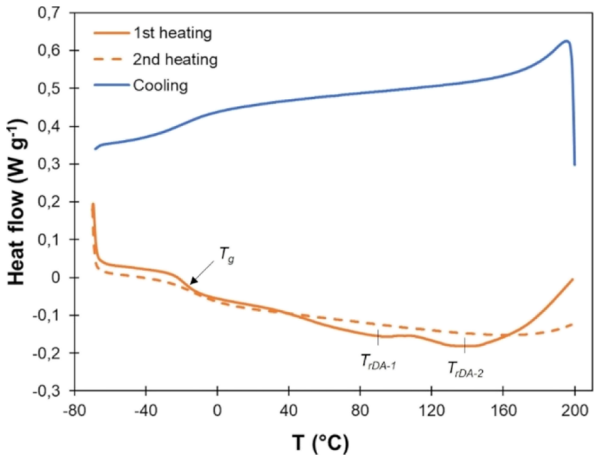

Figure 5. DSC traces of material PI-BM-0.3.

On the first heating run, broad endotherms related to the retro-DA reaction are visible at higher temperature (Figure 5). They can be assigned to the retro-DA of endo (T_{rDA-1}) and exo adducts (T_{rDA-2}), occurring around 90 and 140 °C, respectively.[56,65] They are no longer visible on the second heating run because the cooling cycle (−10 °C min^{-1}) was too fast to allow for the reformation of the DA adducts. At higher temperature, above 160 °C, the heat flow increases significantly during the first heating run. It can be caused by the exothermic homopolymerization of BM,[66] which has been shown to occur above 150 °C.[63]

DMA was then performed up to 100 °C (Figure 6). Within this temperature range, below the retro-DA reaction, the materials behave as crosslinked networks, with a constant plateau modulus. The plateau modulus increases with the amount of BM because of an increase in crosslink density. Interestingly, T_α follows a completely different trend than T_g measured by DSC (Table 1). It increases from −16 to 9 °C when the amount of BM increases from 0.1 to 0.5 equiv, following the increase in crosslink density. Then, we can hypothesize that in this case, T_g and T_α do not refer to the same part of the material. T_g corresponds to "soft segments," whereas T_α is related to crosslinked domains. This particular phenomenon has already been seen in the case of some polyurethanes for instance, where the mobilities of soft and hard segments are represented by the T_g and T_ω, respectively, with different trends.[67]

Viscoelastic Properties of the Dually Crosslinked CANs. Stress relaxation experiments were performed to study the flow behavior of the dually crosslinked networks. All the materials quickly and fully relax stress, as shown on the normalized stress relaxation curves measured between 25 and 65 °C, which are depicted in Figure 7. They were successfully fitted with a stretched exponential model normalized at 1 s, according to eq 1:[68,69]

$$\frac{G(t)}{G_{1s}} = \exp\left[\left(\frac{1}{\tau^*}\right)^\beta - \left(\frac{t}{\tau^*}\right)^\beta\right] \quad (1)$$

where τ^* is the relaxation time, and β ($0 < \beta < 1$) is a factor characterizing the breadth of the distribution of relaxation times. The fitted curves are presented in Figure 2 as dotted lines. Details of the fitting parameters are given in the Supporting Information.

For a stretched exponential decay, the average relaxation time $\langle\tau\rangle$ is given by[70,71]

https://doi.org/10.1021/acssuschemeng.2c05956
ACS Sustainable Chem. Eng. 2023, 11, 2334−2344

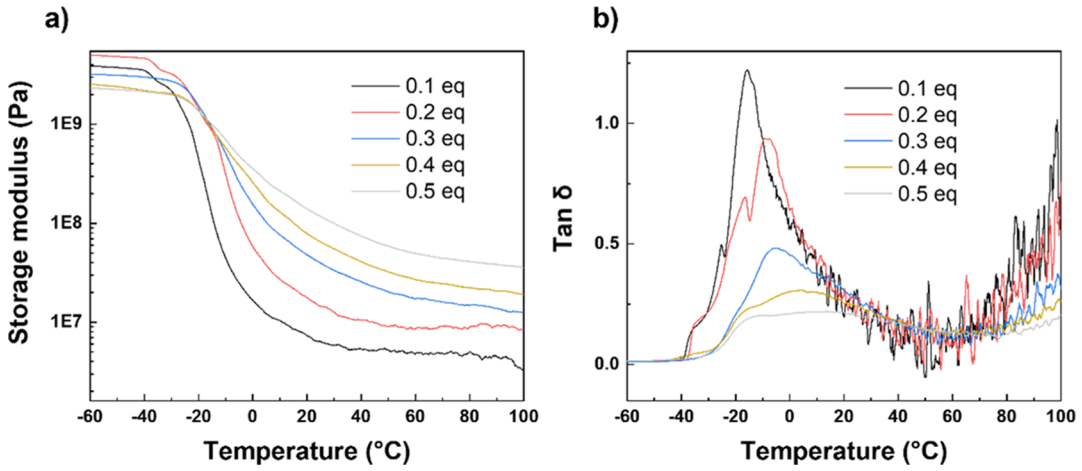

Figure 6. DMA analysis of the materials depending on the BM content: (a) storage modulus and (b) tan δ.

$$\langle\tau\rangle = \frac{\tau^*\Gamma\left(\frac{1}{\beta}\right)}{\beta} \quad (2)$$

Figure 7f shows the Arrhenius plots of the average relaxation times $\langle\tau\rangle$. Plots of $\ln\langle\tau\rangle = f(1000/T)$ are straight lines with $R^2 > 0.99$ for all the materials, indicating that the relaxation time follows an Arrhenius law, one of the characteristic features of vitrimer materials:

$$\langle\tau\rangle = Ae^{-E_a/RT} \quad (3)$$

with E_a the activation energy.

The relaxation times increase with the amount of BM used for crosslinking by DA because of the increased crosslink density of the materials. All materials show similar activation energies, with an average of 93 ± 6 kJ mol^{-1}. It is in the same range as previously reported for other PI vitrimers based on oligo-ether-amines with similar crosslink densities.[43]

The parameter β obtained from the fits (eq 1) characterizes the breadth of the distribution of relaxation times. $\beta = 1$ indicates a single relaxation time, corresponding to a Maxwell model, whereas decreasing β corresponds to broader distributions. Here, β was found to decrease significantly when the amount of BM increases (Figure 8), indicating a broader distribution of relaxations when the crosslinking by DA adducts increases. The values obtained for high crosslinking density are very low (β = 0.24 ± 0.04 for 0.5 equiv BM) as compared to other reported values. In CANs based on a single type of dynamic bond, β values are generally between 0.7 and 0.9.[68,69,71−73] Lower values were reported for block copolymer vitrimers (0.45 to 0.59)[74] or for dissociative CANs based on amide−imide exchanges (0.13 to 0.58).[75] In the latter, the extremely low values of β were explained by the occurrence of other relaxation modes in addition to bond exchange by transamidation, involving, for instance, the dissociation of hydrogen bonds. Here, the decrease of β when the amount of DA adducts in the network increases suggests the potential role of retro-DA/DA reactions in the relaxation process in addition to imine exchanges, although the studied temperature range is far below the expected temperature of the retro-DA reaction.[39] Indeed, networks only based on DA adducts between furans and maleimides were shown to fully relax stress in the 60−90 °C range because the dynamic equilibrium allows for the exchange of covalent bonds within the network, although the equilibrium strongly favors the coupling reaction.[76]

To study the bond exchange at higher temperature, PI-BM-0.3 was subjected to frequency sweeps from 80 to 120 °C. The results are presented in Figure 9. Up to 100 °C, a constant rubbery plateau is observed. It means that in this temperature range, the DA-retro-DA equilibrium is clearly shifted toward the DA reaction, leading to constant crosslink density. Imine exchange led to a transition from rubbery to liquid state at low frequency, characterized by the crossover between G' and G''. Increasing the temperature leads to a shift in the crossover frequency toward higher values. This behavior corresponds to what is typically observed in associative CANs.[72,77]

Further increasing the temperature progressively leads to a shift in equilibrium of the DA reaction toward the retro reaction. Above 100 °C, a decrease in the rubbery plateau is shown, indicating a reduction of the crosslink density due to the dissociation of the DA adducts. Above this temperature, the materials thus exhibit a change in behavior from associative to dissociative exchanges.

Mechanical Properties and Recycling of Materials. Mechanical properties of the materials were evaluated by uniaxial tensile tests. Representative stress−strain curves are presented in Figure 10, whereas the average values of Young's modulus, tensile strength, and elongation at break are given in Table 2. The properties are directly correlated to the amount of BM used for crosslinking. Increasing the BM content leads to an increase in the crosslink density, resulting in an increase in tensile strength and Young's modulus and a conventional decrease in elongation at break. An optimum in tensile strength is observed for 0.4 equiv BM.

The possibility of recycling the materials by thermal reprocessing was evaluated on PI-BM-0.3. After two reprocessing cycles, the elastic properties are fully preserved (Figure 10b and Table 2). These evolutions show the good potential of recyclability of these sustainable and renewable CAN materials.

CONCLUSIONS

Different CANs combining dynamic associative imine bonds with dissociative DA adducts have been successfully synthesized. These macromolecular architectures are constituted by a linear PI backbone containing a furan moiety that has been crosslinked by DA reactions. Both dynamic bonds were generated from a single biobased building block, FDC, exploiting its aldehyde

https://doi.org/10.1021/acssuschemeng.2c05956
ACS Sustainable Chem. Eng. 2023, 11, 2334−2344

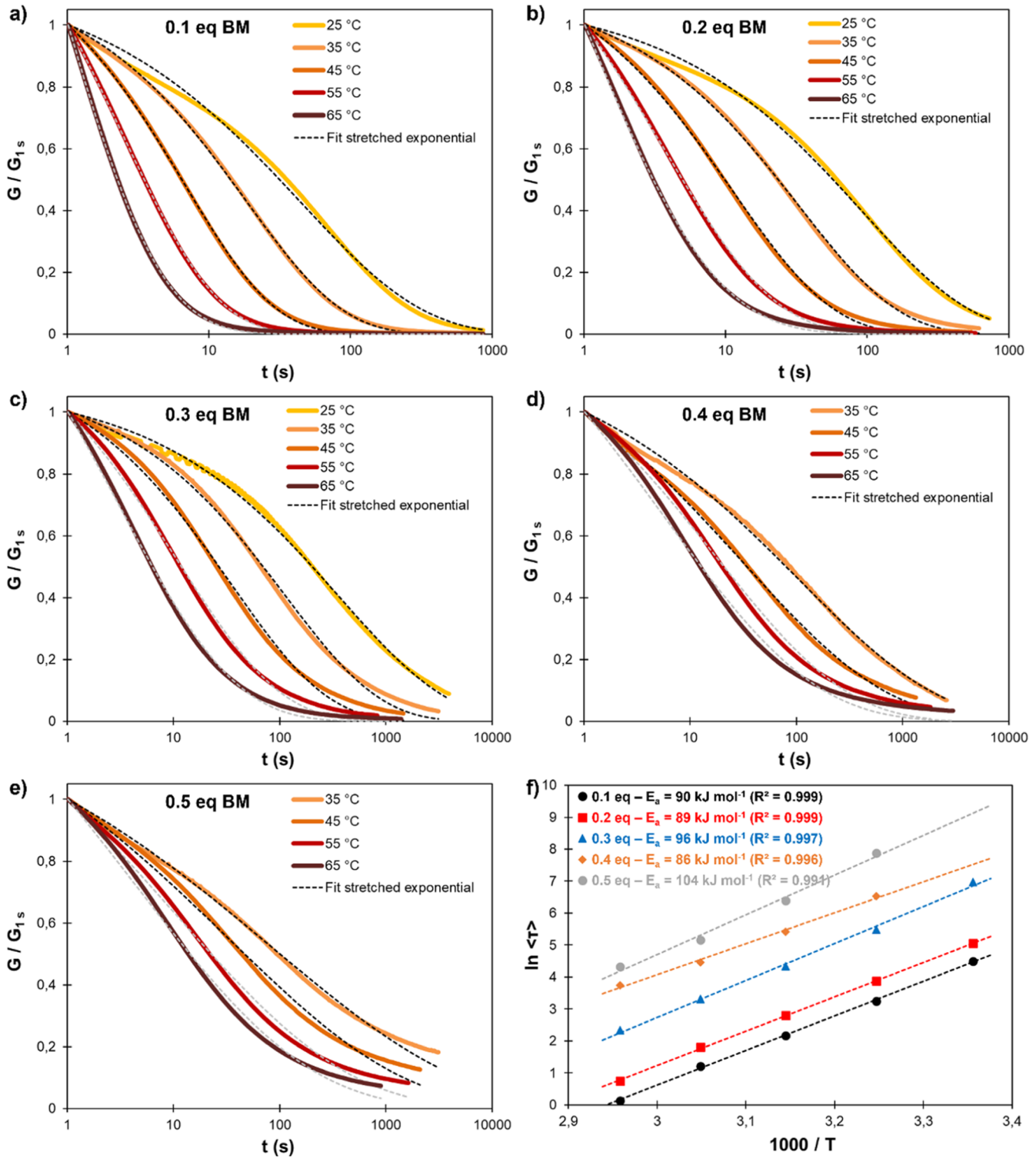

Figure 7. (a–e) Normalized stress relaxation curves of materials prepared from PI and 0.1 to 0.5 equiv of BM. Experimental curves (solid lines) have been fitted (dashed lines) with a stretch exponential model (eq 1). (f) Arrhenius plots of the average relaxation times $\langle\tau\rangle$ calculated from eq 2, as obtained from the fitted data.

functions for the generation of Schiff base linkages by condensation with a diamine and its furan core for DA reaction with a bismaleimide. The peculiar chemical environment of the furan ring, which is surrounded by two electron-donating imine groups, leads to an extremely fast DA coupling with maleimide, substantially faster than what was reported previously for other polymers in the literature. Complete DA reaction was achieved in 1 h on model compounds, and gels were obtained in only 2 h in the case of the full systems.

The dually crosslinked CAN exhibit tunable physical properties depending on the amount of bismaleimide used for crosslinking. Increasing the crosslink density leads to an increase in the T_{α}, tensile strength, and Young's modulus. Interestingly, DMA and frequency sweep experiments show that up to a

https://doi.org/10.1021/acssuschemeng.2c05956
ACS Sustainable Chem. Eng. 2023, 11, 2334–2344

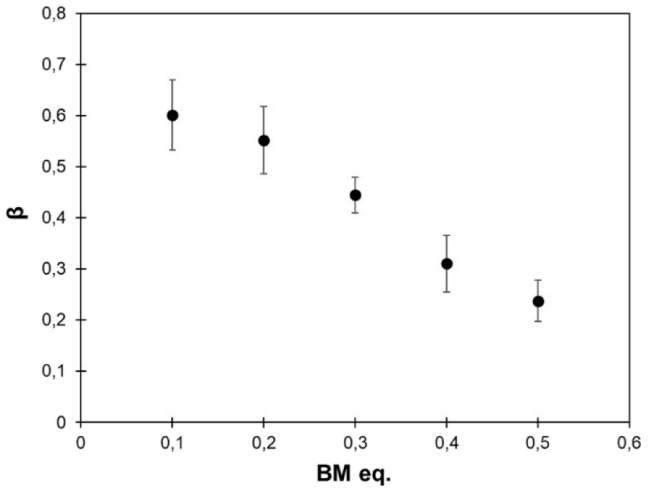

Figure 8. Evolution of the parameter β obtained from the fits of the relaxation data (eq 1) with the amount of BM used for crosslinking by DA reaction.

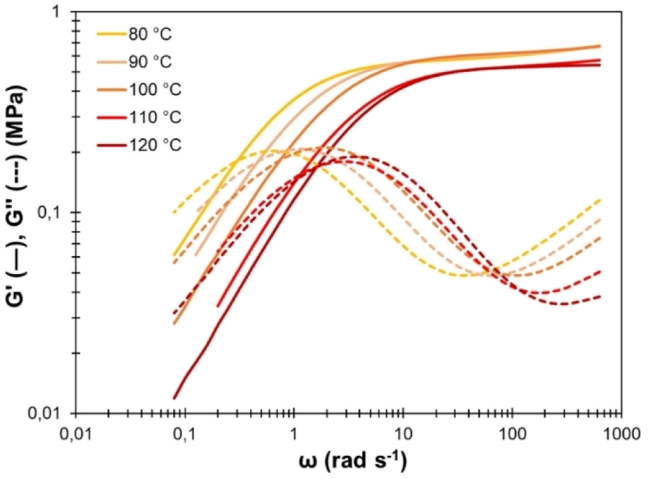

Figure 9. Frequency sweep measurements of material PI-BM-0.3 between 80 and 120 °C.

temperature of 100 °C, a constant rubbery plateau is observed, but that bond reshuffling allows for fast stress relaxation. It means that in this temperature range, the material has a vitrimer-like behavior where the bond exchange is predominantly caused by imine exchanges. At higher temperatures, retro-DA reactions lead to a decrease in the rubbery modulus, indicating a loss of network integrity, a behavior commonly observed in dissociative CANs. Stress relaxation experiments reveal a very broad distribution of relaxations in the materials, which increase with the amount of DA adducts. It suggests that DA/retro-DA exchanges could take part in the stress relaxation process also at temperatures much lower than the temperature of the retro-DA reaction. Since the materials quickly relax stress even close to room temperature, they would inevitably be subjected to creep, which might limit their applications. Introducing nondynamic linkages in the networks,[70] increasing the crosslink density,[43] or reversibly trapping the free amine groups[78] could be different strategies to limit this phenomenon.

The combination of two kinds of dynamic linkages and their potential synergistic effect permits fast reprocessability of the network at low temperature and a preservation of the mechanical properties in the solid state after two reprocessing cycles.

This work opens a great number of perspectives in terms of scientific knowledge, the first of which is represented by decreasing the number of synthetic steps to obtain DDN by using one simple monomer. Furthermore, this work extends the potential applications of an important biobased building block platform: FDC, which precursor was selected in 2004 among the 12 top biobased chemical by the American Department of Energy (DoE).[44]

Table 2. Tensile Strength, Elongation at Break, and Young's Modulus of all the Materials and of PI-BM-0.3 After Two Reprocessing Cycles

Material	Tensile strength (MPa)	Elongation at break (%)	Young's modulus (MPa)
PI-BM-0.1	0.2 ± 0.1	198 ± 3	0.8 ± 0.1
PI-BM-0.2	1.1 ± 0.1	87 ± 9	2.5 ± 0.1
PI-BM-0.3	3.4 ± 0.2	61 ± 5	9.4 ± 0.3
PI-BM-0.4	5.1 ± 0.6	37 ± 1	34.8 ± 1.6
PI-BM-0.5	3.7 ± 0.7	14 ± 5	60.0 ± 0.6
	Recycling Test		
PI-BM-0.3−1°recycle	3.1 ± 0.4	66 ± 10	10.4 ± 1.0
PI-BM-0.3−2°recycle	3.2 ± 0.3	62 ± 7	10.2 ± 0.9

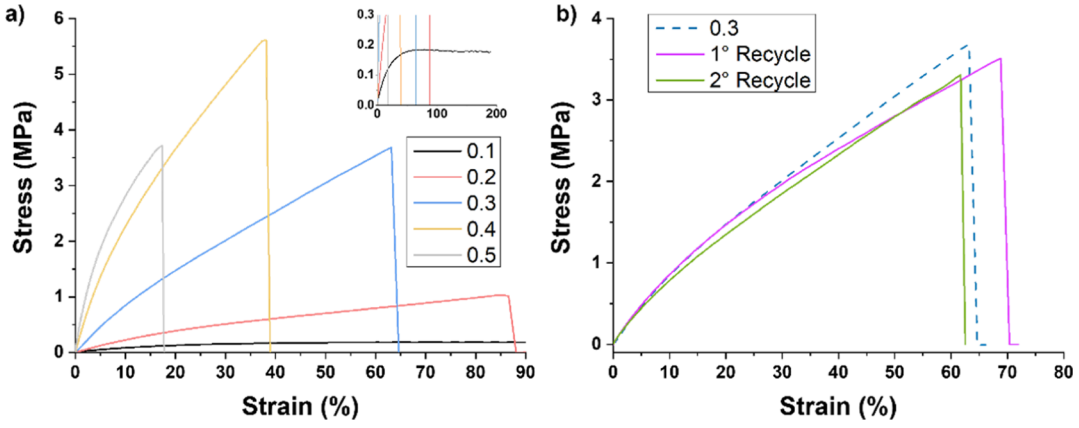

Figure 10. Stress−strain curves of (a) PI-BM at different ratios of BM (magnification of PI-BM-0.1 is reported on the top right for a clearest reading); (b) PI-BM-0.3 before and first and second reprocessing cycles.

https://doi.org/10.1021/acssuschemeng.2c05956
ACS Sustainable Chem. Eng. 2023, 11, 2334−2344

■ ASSOCIATED CONTENT

Supporting Information

The Supporting Information is available free of charge at https://pubs.acs.org/doi/10.1021/acssuschemeng.2c05956.

Synthesis and NMR spectra of model compounds and mechanical characterization of the materials synthesized in this work (PDF)

■ AUTHOR INFORMATION

Corresponding Authors

Antoine Duval − *BioTeam/ICPEES-ECPM, UMR CNRS 7515, Université de Strasbourg, 67087 Strasbourg Cedex 2, France; Soprema, 67025 Strasbourg, France;* orcid.org/0000-0002-6161-8379; Email: antoine.duval@unistra.fr

Luc Averous − *BioTeam/ICPEES-ECPM, UMR CNRS 7515, Université de Strasbourg, 67087 Strasbourg Cedex 2, France;* orcid.org/0000-0002-2797-226X; Email: luc.averous@unistra.fr

Author

Matteo Andrea Lucherelli − *BioTeam/ICPEES-ECPM, UMR CNRS 7515, Université de Strasbourg, 67087 Strasbourg Cedex 2, France;* Present Address: Instituto de Ciencia Molecular (ICMol), Universitat de Valencia, Carrer del Catedrátic José Beltrán Martinez, 2, 46980 Paterna (Valencia, Spain); orcid.org/0000-0003-1055-3269

Complete contact information is available at: https://pubs.acs.org/10.1021/acssuschemeng.2c05956

Funding

Part of this work was funded by Grand Est-region in France within the MIPPI-4D project.

Notes

The authors declare no competing financial interest.

■ ACKNOWLEDGMENTS

The authors acknowledge Dr. Alfred Bazin for his help developing a script for the fast extrapolation of Young's modulus values.

■ REFERENCES

(1) Scott, T. F.; Schneider, A. D.; Cook, W. D.; Bowman, C. N. Photoinduced Plasticity in Cross-Linked Polymers. *Science* **2005**, *308*, 1615−1617.

(2) Kloxin, C. J.; Scott, T. F.; Adzima, B. J.; Bowman, C. N. Covalent Adaptable Networks (CANs): A Unique Paradigm in Cross-Linked Polymers. *Macromolecules* **2010**, *43*, 2643−2653.

(3) Bowman, C. N.; Kloxin, C. J. Covalent Adaptable Networks: Reversible Bond Structures Incorporated in Polymer Networks. *Angew. Chem., Int. Ed.* **2012**, *51*, 4272−4274.

(4) Kloxin, C. J.; Bowman, C. N. Covalent Adaptable Networks: Smart, Reconfigurable and Responsive Network Systems. *Chem. Soc. Rev.* **2013**, *42*, 7161−7173.

(5) Scheutz, G. M.; Lessard, J. J.; Sims, M. B.; Sumerlin, B. S. Adaptable Crosslinks in Polymeric Materials: Resolving the Intersection of Thermoplastics and Thermosets. *J. Am. Chem. Soc.* **2019**, *141*, 16181−16196.

(6) Winne, J. M.; Leibler, L.; Du Prez, F. E. D. Dynamic Covalent Chemistry in Polymer Networks: A Mechanistic Perspective. *Polym. Chem.* **2019**, *10*, 6091−6108.

(7) Montarnal, D.; Capelot, M.; Tournilhac, F.; Leibler, L. Silica-Like Malleable Materials from Permanent Organic Networks. *Science* **2011**, *334*, 965−968.

(8) Capelot, M.; Montarnal, D.; Tournilhac, F.; Leibler, L. Metal-Catalyzed Transesterification for Healing and Assembling of Thermosets. *J. Am. Chem. Soc.* **2012**, *134*, 7664−7667.

(9) Capelot, M.; Unterlass, M. M.; Tournilhac, F.; Leibler, L. Catalytic Control of the Vitrimer Glass Transition. *ACS Macro Lett.* **2012**, *1*, 789−792.

(10) Denissen, W.; Winne, J. M.; Du Prez, F. E. D. Vitrimers: Permanent Organic Networks with Glass-like Fluidity. *Chem. Sci.* **2015**, *7*, 30−38.

(11) Van Zee, N. J.; Nicolaÿ, R. Vitrimers: Permanently crosslinked polymers with dynamic network topology. *Prog. Polym. Sci.* **2020**, *104*, 101233.

(12) Elling, B. R.; Dichtel, W. R. Reprocessable Cross-Linked Polymer Networks: Are Associative Exchange Mechanisms Desirable? *ACS Cent. Sci.* **2020**, *6*, 1488−1496.

(13) Porath, L.; Soman, B.; Jing, B. B.; Evans, C. M. Vitrimers: Using Dynamic Associative Bonds to Control Viscoelasticity, Assembly, and Functionality in Polymer Networks. *ACS Macro Lett.* **2022**, *11*, 475−483.

(14) Podgórski, M.; Fairbanks, B. D.; Kirkpatrick, B. E.; McBride, M.; Martinez, A.; Dobson, A.; Bongiardina, N. J.; Bowman, C. N. Toward Stimuli-Responsive Dynamic Thermosets through Continuous Development and Improvements in Covalent Adaptable Networks (CANs). *Adv. Mater.* **2020**, *32*, 1906876.

(15) Zhu, Y.; Zhang, J.; Wu, Q.; Chen, M.; Huang, G.; Zheng, J.; Wu, J. Three-Dimensional Programmable, Reconfigurable, and Recyclable Biomass Soft Actuators Enabled by Designing an Inverse Opal-Mimetic Structure with Exchangeable Interfacial Crosslinks. *ACS Appl. Mater. Interfaces* **2020**, *12*, 15757−15764.

(16) Zheng, N.; Xu, Y.; Zhao, Q.; Xie, T. Dynamic Covalent Polymer Networks: A Molecular Platform for Designing Functions beyond Chemical Recycling and Self-Healing. *Chem. Rev.* **2021**, *121*, 1716−1745.

(17) Fortman, D. J.; Brutman, J. P.; De Hoe, G. X.; Snyder, R. L.; Dichtel, W. R.; Hillmyer, M. A. Approaches to Sustainable and Continually Recyclable Cross-Linked Polymers. *ACS Sustainable Chem. Eng.* **2018**, *6*, 11145−11159.

(18) Hayashi, M. Implantation of Recyclability and Healability into Cross-Linked Commercial Polymers by Applying the Vitrimer Concept. *Polymers* **2020**, *12*, 1322.

(19) Lucherelli, M. A.; Duval, A.; Avérous, L. Biobased Vitrimers: Towards Sustainable and Adaptable Performing Polymer Materials. *Prog. Polym. Sci.* **2022**, *127*, 101515.

(20) Denissen, W.; Droesbeke, M.; Nicolaÿ, R.; Leibler, L.; Winne, J. M.; Du Prez, F. E. Chemical Control of the Viscoelastic Properties of Vinylogous Urethane Vitrimers. *Nat. Commun.* **2017**, *8*, 14857.

(21) Cuminet, F.; Caillol, S.; Dantras, É.; Leclerc, É.; Ladmiral, V. Neighboring Group Participation and Internal Catalysis Effects on Exchangeable Covalent Bonds: Application to the Thriving Field of Vitrimer Chemistry. *Macromolecules* **2021**, *54*, 3927−3961.

(22) Guerre, M.; Taplan, C.; Winne, J. M.; Du Prez, F. E. D. Vitrimers: Directing Chemical Reactivity to Control Material Properties. *Chem. Sci.* **2020**, *11*, 4855−4870.

(23) Jiang, Z.; Bhaskaran, A.; Aitken, H. M.; Shackleford, I. C. G.; Connal, L. A. Using Synergistic Multiple Dynamic Bonds to Construct Polymers with Engineered Properties. *Macromol. Rapid Commun.* **2019**, *40*, 1900038.

(24) Hammer, L.; Van Zee, N. J.; Nicolaÿ, R. Dually Crosslinked Polymer Networks Incorporating Dynamic Covalent Bonds. *Polymers* **2021**, *13*, 396.

(25) Jackson, A. W.; Fulton, D. A. Triggering Polymeric Nanoparticle Disassembly through the Simultaneous Application of Two Different Stimuli. *Macromolecules* **2012**, *45*, 2699−2708.

(26) Lv, C.; Zhao, K.; Zheng, J. A Highly Stretchable Self-Healing Poly(Dimethylsiloxane) Elastomer with Reprocessability and Degradability. *Macromol. Rapid Commun.* **2018**, *39*, 1700686.

(27) Fortman, D. J.; Snyder, R. L.; Sheppard, D. T.; Dichtel, W. R. Rapidly Reprocessable Cross-Linked Polyhydroxyurethanes Based on Disulfide Exchange. *ACS Macro Lett.* **2018**, *7*, 1226−1231.

(28) Chen, M.; Zhou, L.; Wu, Y.; Zhao, X.; Zhang, Y. Rapid Stress Relaxation and Moderate Temperature of Malleability Enabled by the Synergy of Disulfide Metathesis and Carboxylate Transesterification in Epoxy Vitrimers. *ACS Macro Lett.* **2019**, *8*, 255−260.
(29) Zhao, S.; Wang, D.; Russell, T. P. Biobased Dynamic Polymer Networks with Rapid Stress Relaxation. *ACS Sustainable Chem. Eng.* **2021**, *9*, 11091−11099.
(30) Yang, X.; Liu, G.; Peng, L.; Guo, J.; Tao, L.; Yuan, J.; Chang, C.; Wei, Y.; Zhang, L. Highly Efficient Self-Healable and Dual Responsive Cellulose-Based Hydrogels for Controlled Release and 3D Cell Culture. *Adv. Funct. Mater.* **2017**, *27*, 1703174.
(31) Cromwell, O. R.; Chung, J.; Guan, Z. Malleable and Self-Healing Covalent Polymer Networks through Tunable Dynamic Boronic Ester Bonds. *J. Am. Chem. Soc.* **2015**, *137*, 6492−6495.
(32) Röttger, M.; Domenech, T.; van der Weegen, R. van der; Breuillac, A.; Nicolaÿ, R.; Leibler, L. High-Performance Vitrimers from Commodity Thermoplastics through Dioxaborolane Metathesis. *Science* **2017**, *356*, 62−65.
(33) Ogden, W. A.; Guan, Z. Recyclable, Strong, and Highly Malleable Thermosets Based on Boroxine Networks. *J. Am. Chem. Soc.* **2018**, *140*, 6217−6220.
(34) Luisier, N.; Schenk, K.; Severin, K. A Four-Component Organogel Based on Orthogonal Chemical Interactions. *Chem. Commun.* **2014**, *50*, 10233−10236.
(35) Delpierre, S.; Willocq, B.; Manini, G.; Lemaur, V.; Goole, J.; Gerbaux, P.; Cornil, J.; Dubois, P.; Raquez, J.-M. Simple Approach for a Self-Healable and Stiff Polymer Network from Iminoboronate-Based Boroxine Chemistry. *Chem. Mater.* **2019**, *31*, 3736−3744.
(36) Li, Y.; Yang, L.; Zeng, Y.; Wu, Y.; Wei, Y.; Tao, L. Self-Healing Hydrogel with a Double Dynamic Network Comprising Imine and Borate Ester Linkages. *Chem. Mater.* **2019**, *31*, 5576.
(37) Collins, J.; Nadgorny, M.; Xiao, Z.; Connal, L. A. Doubly Dynamic Self-Healing Materials Based on Oxime Click Chemistry and Boronic Acids. *Macromol. Rapid Commun.* **2017**, *38*, 1600760.
(38) Wang, Y.; Yu, H.; Yang, H.; Hao, X.; Tang, Q.; Zhang, X. An Injectable Interpenetrating Polymer Network Hydrogel with Tunable Mechanical Properties and Self-Healing Abilities. *Macromol. Chem. Phys.* **2017**, *218*, 1700348.
(39) Gandini, A. The Furan/Maleimide Diels−Alder Reaction: A Versatile Click−Unclick Tool in Macromolecular Synthesis. *Prog. Polym. Sci.* **2013**, *38*, 1−29.
(40) Xu, X.; Ma, S.; Wang, S.; Wang, B.; Feng, H.; Li, P.; Liu, Y.; Yu, Z.; Zhu, J. Fast-Reprocessing, Postadjustable, Self-Healing Covalent Adaptable Networks with Schiff Base and Diels-Alder Adduct. *Macromol. Rapid Commun.* **2022**, *43*, 2100777.
(41) Yu, F.; Cao, X.; Du, J.; Wang, G.; Chen, X. Multifunctional Hydrogel with Good Structure Integrity, Self-Healing, and Tissue-Adhesive Property Formed by Combining Diels-Alder Click Reaction and Acylhydrazone Bond. *ACS Appl. Mater. Interfaces* **2015**, *7*, 24023−24031.
(42) Dhers, S.; Vantomme, G.; Avérous, L. A Fully Bio-Based Polyimine Vitrimer Derived from Fructose. *Green Chem.* **2019**, *21*, 1596−1601.
(43) Hajj, R.; Duval, A.; Dhers, S.; Avérous, L. Network Design to Control Polyimine Vitrimer Properties: Physical Versus Chemical Approach. *Macromolecules* **2020**, *53*, 3796−3805.
(44) Werpy, T.; Petersen, G.*Top Value Added Chemicals from Biomass: Volume I -- Results of Screening for Potential Candidates from Sugars and Synthesis Gas*; DOE/GO-102004-1992; National Renewable Energy Lab: Golden, CO (US), 2004.
(45) Nie, J.; Xie, J.; Liu, H. Activated Carbon-Supported Ruthenium as an Efficient Catalyst for Selective Aerobic Oxidation of 5-Hydroxymethylfurfural to 2,5-Diformylfuran. *Chin. J. Catal.* **2013**, *34*, 871−875.
(46) Chatterjee, M.; Ishizaka, T.; Chatterjee, A.; Kawanami, H. Dehydrogenation of 5-Hydroxymethylfurfural to Diformylfuran in Compressed Carbon Dioxide: An Oxidant Free Approach. *Green Chem.* **2017**, *19*, 1315−1326.
(47) Al Ghatta, A.; Wilton-Ely, J. D. E. T.; Hallett, J. P. Efficient Formation of 2,5-Diformylfuran in Ionic Liquids at High Substrate Loadings and Low Oxygen Pressure with Separation through Sublimation. *ACS Sustainable Chem. Eng.* **2020**, *8*, 2462−2471.
(48) Kisszekelyi, P.; Hardian, R.; Vovusha, H.; Chen, B.; Zeng, X.; Schwingenschlögl, U.; Kupai, J.; Szekely, G. Selective Electrocatalytic Oxidation of Biomass-Derived 5-Hydroxymethylfurfural to 2,5-Diformylfuran: from Mechanistic Investigations to Catalyst Recovery. *ChemSusChem* **2020**, *13*, 3127−3136.
(49) Millán Acosta, A.; Cuesta Turull, C.; Cosovanu, D.; Sala Martí, N.; Canela-Garayoa, R. Novel and Efficient Biotechnological Approach to Produce 2,5-Diformylfuran from Biomass-Derived 5-Hydroxymethylfurfural. *ACS Sustainable Chem. Eng.* **2021**, *9*, 14550−14558.
(50) Dai, J. Synthesis of 2,5-Diformylfuran from Renewable Carbohydrates and Its Applications: A Review. *Green Energy Environ.* **2021**, *6*, 22−32.
(51) Hoang Tran, P. Recent Approaches in the Catalytic Transformation of Biomass-Derived 5-Hydroxymethylfurfural into 2,5-Diformylfuran. *ChemSusChem* **2022**, *15*, No. e202200220.
(52) van Putten, R.-J.; van der Waal, J. C.; de Jong, E.; Rasrendra, C. B.; Heeres, H. J.; de Vries, J. G. Hydroxymethylfurfural, A Versatile Platform Chemical Made from Renewable Resources. *Chem. Rev.* **2013**, *113*, 1499−1597.
(53) Zhang, D.; Dumont, M.-J. Advances in Polymer Precursors and Bio-Based Polymers Synthesized from 5-Hydroxymethylfurfural. *J. Polym. Sci., Part A: Polym. Chem.* **2017**, *55*, 1478−1492.
(54) Galkin, K. I.; Ananikov, V. P. When Will 5-Hydroxymethylfurfural, the "Sleeping Giant" of Sustainable Chemistry, Awaken? *ChemSusChem* **2019**, *12*, 2976−2982.
(55) Laugel, C.; Lebras, J.; Marinkovic, S.; Muzart, J.; Estrine, B.; Hoffmann, N.Procede de fabrication de furane 2,5-dicarboxaldehyde a partir d'hydroxymethylfurfural et de ses derives halogenes n'utilisant pas de catalyseur metallique, FR 3008409 A1, January 16, 2015. https://data.inpi.fr/brevets/FR3008409?lng=en.
(56) Froidevaux, V.; Borne, M.; Laborbe, E.; Auvergne, R.; Gandini, A.; Boutevin, B. Study of the Diels-Alder and retro-Diels-Alder reaction between furan derivatives and maleimide for the creation of new materials. *RSC Adv.* **2015**, *5*, 37742−37754.
(57) Tremblay-Parrado, K. K.; Avérous, L. Renewable Responsive Systems Based on Original Click and Polyurethane Cross-Linked Architectures with Advanced Properties. *ChemSusChem* **2020**, *13*, 238−251.
(58) Tremblay-Parrado, K.-K.; Avérous, L. Synthesis and Behavior of Responsive Biobased Polyurethane Networks Cross-Linked by Click Chemistry: Effect of the Cross-Linkers and Backbone Structures. *Eur. Polym. J.* **2020**, *135*, 109840.
(59) Tremblay-Parrado, K.-K.; García-Astrain, C.; Avérous, L. Click Chemistry for the Synthesis of Biobased Polymers and Networks Derived from Vegetable Oils. *Green Chem.* **2021**, *23*, 4296−4327.
(60) García-Astrain, C.; Gandini, A.; Coelho, D.; Mondragon, I.; Retegi, A.; Eceiza, A.; Corcuera, M. A.; Gabilondo, N. Green chemistry for the synthesis of methacrylate-based hydrogels crosslinked through Diels-Alder reaction. *Eur. Polym. J.* **2013**, *49*, 3998−4007.
(61) Cioc, R. C.; Crockatt, M.; van der Waal, J. C.; Bruijnincx, P. C. A. The Interplay between Kinetics and Thermodynamics in Furan Diels-Alder Chemistry for Sustainable Chemicals Production. *Angew. Chem., Int. Ed.* **2022**, *61*, No. e202114720.
(62) Khan, T. S.; Gupta, S.; Ahmad, M.; Alam, M. I.; Haider, M. A. Effect of substituents and promoters on the Diels-Alder cycloaddition reaction in the biorenewable synthesis of trimellitic acid. *RSC Adv.* **2020**, *10*, 30656−30670.
(63) Orozco, F.; Niyazov, Z.; Garnier, T.; Migliore, N.; Zdvizhkov, A. T.; Raffa, P.; Moreno-Villoslada, I.; Picchioni, F.; Bose, R. K. Maleimide Self-Reaction in Furan/Maleimide-Based Reversibly Crosslinked Polyketones: Processing Limitation or Potential Advantage? *Molecules* **2021**, *26*, 2230.
(64) Duval, A.; Sarbu, A.; Dalmas, F.; Albertini, D.; Avérous, L. 2,3-Butanediol as a Biobased Chain Extender for Thermoplastic Polyur-

ethanes: Influence of Stereochemistry on Macromolecular Architectures and Properties. *Macromolecules* **2022**, *55*, 5371−5381.
(65) Duval, A.; Couture, G.; Caillol, S.; Avérous, L. Biobased and Aromatic Reversible Thermoset Networks from Condensed Tannins via the Diels−Alder Reaction. *ACS Sustainable Chem. Eng.* **2017**, *5*, 1199−1207.
(66) Mison, P.; Sillion, B.Thermosetting Oligomers Containing Maleimides and Nadimides End-Groups. In *Progress in Polyimide Chemistry I*; Kricheldorf, H. R., Ed.; *Advances in Polymer Science*; Springer: Berlin, Heidelberg, 1999; pp 137−179.
(67) Laurichesse, S.; Huillet, C.; Avérous, L. Original Polyols Based on Organosolv Lignin and Fatty Acids: New Bio-Based Building Blocks for Segmented Polyurethane Synthesis. *Green Chem.* **2014**, *16*, 3958−3970.
(68) Majumdar, S.; Zhang, H.; Soleimani, M.; van Benthem, R. A. T. M.; Heuts, J. P. A.; Sijbesma, R. P. Phosphate Triester Dynamic Covalent Networks. *ACS Macro Lett.* **2020**, *9*, 1753−1758.
(69) Majumdar, S.; Mezari, B.; Zhang, H.; van Aart, J.; van Benthem, R. A. T. M.; Heuts, J. P. A.; Sijbesma, R. P. Efficient Exchange in a Bioinspired Dynamic Covalent Polymer Network via a Cyclic Phosphate Triester Intermediate. *Macromolecules* **2021**, *54*, 7955−7962.
(70) Li, L.; Chen, X.; Jin, K.; Torkelson, J. M. Vitrimers Designed Both To Strongly Suppress Creep and To Recover Original Cross-Link Density after Reprocessing: Quantitative Theory and Experiments. *Macromolecules* **2018**, *51*, 5537−5546.
(71) Li, L.; Chen, X.; Torkelson, J. M. Reprocessable Polymer Networks via Thiourethane Dynamic Chemistry: Recovery of Cross-Link Density after Recycling and Proof-of-Principle Solvolysis Leading to Monomer Recovery. *Macromolecules* **2019**, *52*, 8207−8216.
(72) Jourdain, A.; Asbai, R.; Anaya, O.; Chehimi, M. M.; Drockenmuller, E.; Montarnal, D. Rheological Properties of Covalent Adaptable Networks with 1,2,3-Triazolium Cross-Links: The Missing Link between Vitrimers and Dissociative Networks. *Macromolecules* **2020**, *53*, 1884−1900.
(73) Self, J. L.; Dolinski, N. D.; Zayas, M. S.; Read de Alaniz, J.; Bates, C. M. Brønsted-Acid-Catalyzed Exchange in Polyester Dynamic Covalent Networks. *ACS Macro Lett.* **2018**, *7*, 817−821.
(74) Lessard, J. J.; Scheutz, G. M.; Sung, S. H.; Lantz, K. A.; Epps, T. H.; Sumerlin, B. S. Block Copolymer Vitrimers. *J. Am. Chem. Soc.* **2020**, *142*, 283−289.
(75) Chen, Y.; Zhang, H.; Majumdar, S.; van Benthem, R. A. T. M.; Heuts, J. P. A.; Sijbesma, R. P. Dynamic Polyamide Networks via Amide-Imide Exchange. *Macromolecules* **2021**, *54*, 9703−9711.
(76) Zhang, G.; Zhao, Q.; Yang, L.; Zou, W.; Xi, X.; Xie, T. Exploring Dynamic Equilibrium of Diels-Alder Reaction for Solid State Plasticity in Remoldable Shape Memory Polymer Network. *ACS Macro Lett.* **2016**, *5*, 805−808.
(77) Taplan, C.; Guerre, M.; Winne, J. M.; Du Prez, F. E. D. Fast Processing of Highly Crosslinked, Low-Viscosity Vitrimers. *Mater. Horiz.* **2020**, *7*, 104−110.
(78) Van Lijsebetten, F.; De Bruycker, K.; Spiesschaert, Y.; Winne, J. M.; Du Prez, F. E. Suppressing Creep and Promoting Fast Reprocessing of Vitrimers with Reversibly Trapped Amines. *Angew. Chem., Int. Ed.* **2022**, *61*, No. e202113872.

https://doi.org/10.1021/acssuschemeng.2c05956
ACS Sustainable Chem. Eng. 2023, 11, 2334−2344